



Research

Identification of *KCNJ5* gene an adverse prognosis associated novel onco-ionchannel in Indian pancreatic cancer cohort

Akash Bararia¹ · Arunima Maiti² · Gourav Ghosh³ · Deepyaman Das⁴ · Debabrata Ghosh Dastidar³ · Sumit Mukherjee^{5,11} · Shibajyoti Ghosh⁶ · Bitan K. Chattopadhyay⁷ · Sudeep Banerjee⁸ · Supriyo Ghatak⁹ · Nilabja Sikdar^{1,10} 

Received: 9 September 2024 / Accepted: 20 February 2025

Published online: 25 February 2025

© The Author(s) 2025 

Abstract

Background Pancreatic cancer (PanCa) is one of the most lethal cancers (survival ~ 12%). As the conventional therapeutic interventions are mostly futile, a deep understanding of the disease pathophysiology is an urgent need. Ion channels, located on cell membrane, contribute significantly to cancer hallmarks, through dysregulation of various ion translocation; however, the fundamental mechanisms remain uncertain.

Methods To identify these oncochannels in Indian cohort of PanCa, we utilized 450 K data, published in our previous study, and identified potential pathways involved. Their expressions were evaluated using TCGA data and an independent Indian paired patient cohort (n = 20). The top genes were further validated using GEO and ScRNA seq dataset. Potential target ability of *KCNJ5* was identified through molecular dynamic based drug designing.

Results A set of 7 differentially methylated and differentially expressed genes of ion-channel proteins namely *KCNJ5*, *CACNB2*, *KCNA3*, *KCNA6*, *RASA3*, *GABBR2* and *CLIC5* were identified in Indian PanCa cohort only. *KCNJ5* was significantly upregulated and associated with worse survival in Indian cohort, whereas downregulated in TCGA and other Caucasians patient populations. Two TFs controlling the *KCNJ5* expression are *POU2F1* and *POU3F1*. Few predicted small molecules targeting *Kcnj5* are, Amiloride, Vernakalant hydrochloride, Dalfampridine, Glyburide and Levromakalim. It also showed notable interactions with a steroidal anticancer agent, protodioscin.

Conclusion An onco-channel gene, *KCNJ5* significantly upregulated, and showing adverse survival in highly expressed *KCNJ5* group in Indian cohort of PanCa, can be targeted with Amiloride, Vernakalant hydrochloride, Dalfampridine, Glyburide Levromakalim and protodioscin. This understanding can lead to novel target identification for PanCa therapy development.

Keywords Pancreatic ductal adenocarcinoma · 450 K methylation array · Enriched Pathways · Inward rectifying potassium channel · Druggable protein · Differntially methylated ion channel

Supplementary Information The online version contains supplementary material available at <https://doi.org/10.1007/s12672-025-02001-8>.

✉ Nilabja Sikdar, snilabja@gmail.com; snilabja@isical.ac.in | ¹Human Genetics Unit, Biological Sciences Division, Indian Statistical Institute, 203, B. T. Road, Kolkata 700108, India. ²Suraksha Diagnostics Pvt Ltd, Newtown, Rajarhat, Kolkata, India. ³Guru Nanak Institute of Pharmaceutical Science and Technology, Kolkata, India. ⁴Department of Zoology, Raiganj University, Raiganj, WB, India. ⁵Cancer Data Science Laboratory, National Cancer Institute, National Institutes of Health (NIH), Bethesda, MD, USA. ⁶Medical College and Hospital, Kolkata, India. ⁷I.P.G.M.E & R and SSKM, Hospital Kolkata, Kolkata, India. ⁸Tata Medical Center, Kolkata, India. ⁹Apollo Multispeciality Hospital, Kolkata, India. ¹⁰Estuarine and Costal Studies Foundation, Howrah, WB 711101, India. ¹¹Department of Computer Science, Ben-Gurion University, Beer-Sheva, Israel.



Abbreviations

PanCa	Pancreatic cancer
PDAC	Pancreatic ductal adenocarcinoma
PanIN	Pancreatic intraepithelial neoplasia
OS	Overall survival
KCNJ5	Potassium Inwardly Rectifying Channel Subfamily J Member 5
DMP	Differentially methylated position
DMGs	Differentially methylated genes
RMSD	Root Mean Square Deviation
RMSF	Root Mean Square Fluctuation
PSA	Polar Surface Area
Rg	Gyration Radius
TCGA	The Cancer Genome Atlas
GTE _x	Genotype-Tissue Expression
CPTAC	Clinical Proteomic Tumor Analysis Consortium
GEPIA	Gene Expression Profiling Interactive Analysis
CCLC	Cancer Cell Line Encyclopedia
GEO	Gene Expression Omnibus
ScRNA-seq	Single-cell RNA Sequencing
GSEA	Gene Set Enrichment Analysis
KEGG	Kyoto Encyclopedia of Genes and Genomes
GO	Gene Ontology
IPA	Ingenuity Pathway Analysis
gDMs	Genes with differential methylation
KCNA6	Potassium Voltage-Gated Channel Subfamily A Member 6
KCNA3	Potassium Voltage-Gated Channel Subfamily A Member 3
CACNB2	Ca ²⁺ Voltage-Gated Channel Auxiliary Subunit Beta 2
RASA3	Ras GTPase-activating protein 3
GABBR2	Gamma-Aminobutyric Acid Type B Receptor Subunit 2
CLICs	Chloride channels
ANO1	Anoctamin 1
CLCA	Calcium activated chloride channel
CLCN1	Chloride channel Kb (CLCNKB) and chloride voltage-gated channel 1
TRP	Transient receptor potential
ASIC	Aid-sensing ion channels
VGSC	Voltages gated sodium channels
AQP4	Aquaporins
CIBERSORT	Cell-type Identification by Estimating Relative Subsets of RNA Transcripts
GO	Gene Ontology
KEGG	Kyoto Encyclopedia of Genes and Genomes
IPA	Ingenuity pathway analysis
GTE _x	Genotype-Tissue Expression
TCGA	The Cancer Genome Atlas
PPI	Protein–protein interaction
DEICG	Differentially expressed ion channel genes
TF	Transcription factor
TAM	Tumor associated macrophage
M1	Pro-inflammatory macrophages
M2	Anti-inflammatory macrophages
M0	Resting macrophage
TNF	Tumor necrosis factors
CMap	Connectivity Map
HGNC	HUGO Gene Nomenclature Committee

DEICGs	Differentially expressed ion channel genes
PPIN	Protein–protein interaction network
FDA	Food and Drug Administration

1 Introduction

As indicated in GLOBOCAN 2020, PanCa is the 12th most common cancer, ranking 7th (4.7%) in terms of global cancer associated mortality. PanCa is one of the tumors with the worst prognosis, and unlike other cancers, few advances have been made in recent years. The only curative option is surgery, but only 15–20% of patients are candidates, with a high risk of relapse. In advanced PanCa there are few first-line treatment options, however, no validated biomarkers for better treatment selection have been identified so far [1–4]. As, standard treatment options of PanCa are mostly inefficient, a finer understanding of the disease pathophysiology is indispensable for efficient disease management.

Ion channels are transmembrane pore-forming proteins, contributing substantially to “hallmarks of cancer”. These ubiquitous proteins with altered expression in cancer, facilitate inward or outward flow of ions, accordingly modifying cellular bio-chemical and electrical properties, ultimately influencing signaling networks associated with gene expression and inter-organelle dialogues [5, 6]. They modify microenvironmental cues, contributing to PanCa aggressiveness through excessive fibrosis, immune invasion, metastasis and drug/ chemo resistance [7, 8]. Several potassium channels overexpressed in PanCa are: (i) inward potassium channel, Kir3 [9]. (ii) calcium activated potassium channel, KCa3.1 [10] (iii) two-pore domain containing K⁺ channel, TWIK-1 and TASK-2, (iv) voltage-gated K⁺ channels, Kv1.3 Kv1.5 and Kv11.1 [11–13] and (v) potassium calcium-activated channel subfamily N member 4, *KCNN4*. Kv10.1, absent in normal pancreas is expressed in PanCa, while Kv7.1 and *KCNE1* are suppressed in pancreatic ductal adenocarcinoma (PDAC). Chloride channels (CLICs) elevated in PanCa cell lines and tumor samples are (i) *CLIC1*, *CLIC2*, and *CLIC3* (ii) calcium activated chloride channel, anoctamin 1 (*ANO1*) and (iii) *TMEM16A* and *TMEM16J*. [11] While (i) *CLIC5* (ii) calcium activated chloride channel, *CLCA-1* [14] (iii) chloride channel Kb (*CLCNKB*) and chloride voltage-gated channel 1 (*CLCN1*) are inhibited in PDAC. Calcium channels, overexpressed in PDAC are (i) transient receptor potential (TRP) channels, *TRPM2*, *TRPM7*, *TRPM8*, *TRPC1*, *TRPC4*, and *TRPC6* (ii) voltage-dependent calcium channels, CaV2.1 and *ORAI1* [15] *TRPM8* facilitates cell-cycle, proliferation and invasion; while inhibits replicative senescence, thereby contributing in pancreatic neoplasm pathogenesis [16]. However, the molecular mechanism and their precise role in PanCa are still blurred.

In this article, the substantially enriched differentially methylated genes (promoter methylation) and their functions as ion channel genes in PanCa in Indian patient cohorts are presented in a sequential manner. We also confirmed these ion-channels' correlation with PanCa survival by validating them across a range of datasets. This ethnicity-specific variation may offer insights into the creation of innovative treatments and improved management of PanCa disease in India, given the clear significance of ion channels in PanCa disease biology.

2 Methods

2.1 Sample collection and ethical clearance

The study is approved by the Institutional Review Board (IRB) of Indian Statistical Institute, Kolkata. The clinical samples were collected only after taking informed consent and was carried out in compliance with the Helsinki Declaration of 1964. Our study included samples of PDAC patients, collected from, Medical College and Hospital, I.P.G.M.E&R and SSKM Hospital, Tata Medical Center and Apollo Multi-speciality Hospital, Kolkata, during 2013–2022. Detailed methods were described in supplemental information section.

2.2 Identification of crucial methylation altered ion transporter signatures

“Ion transporter” identified as the most enriched term through Metascape, of 91 significant gDMs in Indian PanCa patient cohort [17]. These 91 DMPs were further analyzed through Ingenuity Pathway Analysis (IPA).

2.3 Cross omic clinical validation of differentially methylated genes from Indian patient

mRNA expression status of gDMs were evaluated using TCGA PAAD and GTEx normal pancreas dataset, followed by their methylation status, using TCGA PAAD methylation array dataset based on Wilcoxon test. Protein levels of gDMs were assessed using Clinical Proteomic Tumor Analysis Consortium (CPTAC) dataset. Their stage-wise mRNA expressions were evaluated using GEPIA in PAAD dataset. Mutational profile of the 7 gDMs were assessed using Cbioportal in TCGA PanCa dataset [18]. Overall survival (OS) of these 7 gDMs were studied using Kaplan–meier survival analysis with TCGA dataset using GEPIA2. Overall survival associated with alcohol consumption was also evaluated for a specific gene. Correlations between gene expression and methylation data from TCGA-PAAD dataset of *KCNJ5* were observed using SMART APP (<http://www.bioinfo-zs.com/smartapp>). The expression value (TPM) and methylation (Beta) value were plotted using Pearson correlation by keeping the aggregation method as mean. Expression profile of *KCNJ5* mRNA in 46 different PanCa cell lines was assessed through The Human Protein Atlas (HPA) (<https://www.proteinatlas.org>). *KCNJ5* methylation pattern across various CpG sites on their respective chromosomes were investigated in 35 PDAC cell lines using Cancer Cell Line Encyclopedia (CCLE) (<https://depmap.org/portal/>). DepMap portal was used to evaluate the degree of methylation across the cell lines at various CpG locations [19, 20].

2.4 Validation of *KCNJ5* expression using independent Indian patient sample cohort

RNA was isolated from tumor and normal tissue samples by RNasey Kit (Qiagen) following manufacturers protocol (Cat No. 74104). cDNA was synthesised by RT-PCR using iTaq Universal SYBR Green Supermix (Bio Rad Life Sciences Research, Cat No. 1725125). Detailed methods are described in the supplemental information section. OS of Indian patients (n = 20) was analyzed using R Studio based Kaplan–meier OS method,

2.5 Immuno profiling of differentially methylated genes

LM22 profile using CIBERSORT was used to obtain the immune profile of *KCNJ5* and *CACNB2* gene to derive correlated expression pattern in immune cells present in tumor microenvironment of PanCa. The LM22 matrix is a file of 547 genes that are capable of differentiating between 22 phenotypes of human hematopoietic cells, such as: NK cells, plasma cells, naïve and memory B cells, myeloid subsets, and seven different types of T cells. CIBERSORT was utilized to estimate the number of immune cells that invade tumors in order to analyze cancer.

2.6 Relevant dataset-based validation of *KCNJ5*'s expression in PanCa

The role of *KCNJ5* was evaluated in few other GEO based PanCa datasets, comprising of, 450 K methylation data: GSE74071 (21 malignant and 7 adjacent normal) and GSE49149 (167 tumors and 27 adjacent normal) and RNA-Seq data: GSE211398 (28 tumor tissues) and GSE16515 (36 Tumor and 16 normal).

2.7 Functional enrichment of *KCNJ5* along with its corelated genes

LinkedOmics, containing multi-omics data from 32 TCGA cancer types, with submodules like, LinkFinder (for gene association) and Link Interpreter (for enrichment analysis) was used to investigate functional and pathway enrichment analysis of *KCNJ5* along with its associated genes in PanCa. GO was done to obtain interaction amongst associated genes using both TCGA PAAD dataset and dataset obtained from our previous study.

2.8 Identification of TFs that regulate *KCNJ5*

The transcription factors (TFs) for *KCNJ5* were identified by combining the ChIP-Seq data based TF binding data of ChEA (<https://maayanlab.cloud/chea3/>) and RegNetwork (<http://www.regnetworkweb.org>) [21]. The common TFs in both the databases for *KCNJ5* were considered in our analysis.

2.9 Analyzing RNA-seq datasets to identify ion channel genes in PDACs

Initially, we combined results from two RNA-seq data sets (GSE211398 and GSE93326) and The Cancer Genome Atlas (TCGA) dataset to generate a list of differentially expressed genes (DEGs) for PDAC. The DEG list was prepared by considering a cut off of adjusted $P < 0.05$ and $|\log_2FC| > 0$. We detected genes by comparing 66 pancreatic epithelial tumor samples with 123 stroma samples in GSE93326. In a similar manner, we compared the transcriptome data of 12 non-tumor samples with 15 PDAC samples to find the genes for GSE211398. To find DEGs in these two datasets, we utilised R 4.4.1 and DEseq2. For DEGs that were present in more than one dataset, we considered their average expression across the datasets. Next, we downloaded a list of 330 ion channel genes from HUGO Gene Nomenclature Committee (HGNC) (<https://www.genenames.org/data/genegroup/#!/group/177>) and then analyzed their gene expression in the screened DEG list to get differentially expressed ion channel genes (DEICGs). Functional enrichment and cluster analysis of the DEICGs was done in Metascape.

2.10 ScRNA data-based screening of methylation-regulated differentially expressed genes

Expression *KCNJ5* was assessed in single cells using scRNA-seq data (PRJCA001063) in the Genome Sequence Archive (24 untreated PDAC tumor samples and 11 controls)[22].

2.11 Identification of small drug molecules targeting *KCNJ5*

The connectivity map (CMap) online dataset (<https://clue.io/about>) was used to identify, FDA approved and unapproved small molecules interacting with *KCNJ5*. Additionally, through depmap portal (<https://depmap.org/portal/>) we identified several compounds targeting *KCNJ5*. These predicted small molecules might be useful for disease management in PanCa.

2.12 Prediction of drugs against *KCNJ5*

Potential drugs against *KCNJ5* were predicted using GDSC1, GDSC2, CTRP, and PRISM databases followed by the method described by Mao et al. [23].

2.13 Virtual screening of potential ligands to *KCNJ5*

We conducted a virtual screening of potential ligands against the *KCNJ5* protein using the Schrödinger suite [24]. Homology models of *KCNJ5* were built with SWISS-MODEL and evaluated using QMEAN. The protein structures were prepped with Maestro. A library of 148 candidate ligands from PubChem was processed with LigPrep and Epik. Docking was performed with Glide's HTVS, SP, and XP modes. Top-ranked complexes underwent 100 ns of molecular dynamics simulation using NAMD to assess stability and dynamics. [25] Detailed protocols were in the Supplementary Information section.

3 Results

3.1 Identification of differentially expressed genes (DEGs) and pathway enrichment analyses

Ninety-one differentially methylated genes (gDMs) of interest, identified in our previous study, were subjected to enrichment of Gene Ontology (GO) terms on biological processes using Metascape. Enrichment pathways in KEGG

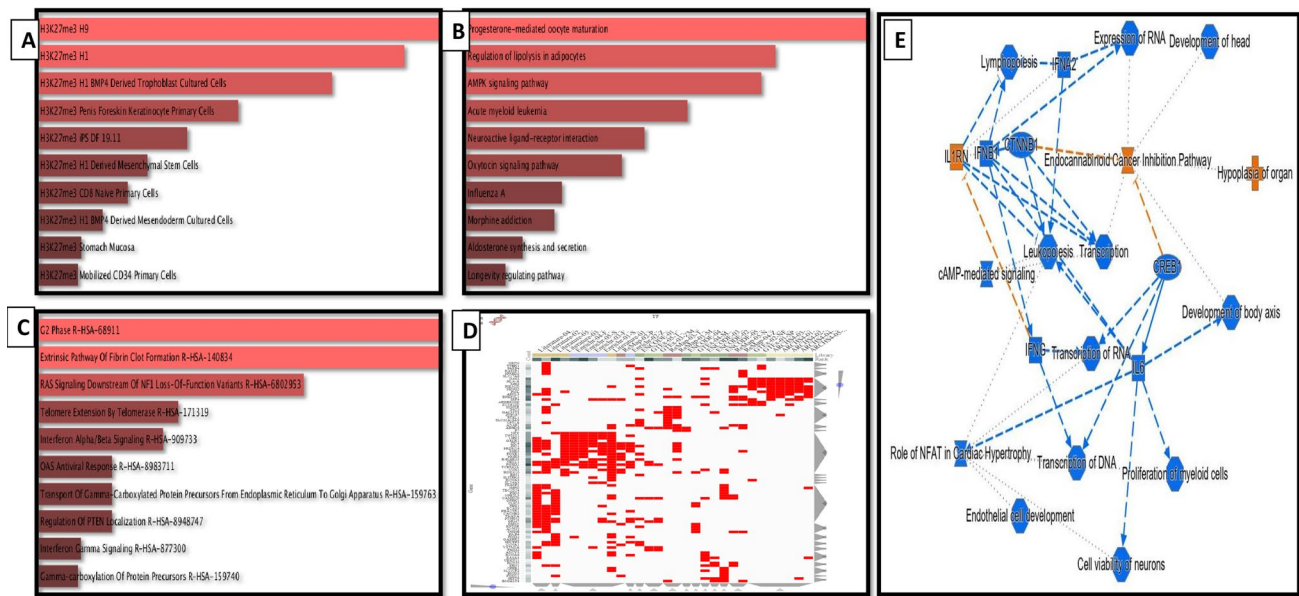


Fig. 1 Pathway associated landscape evaluation: Differentially methylated 91 gene signature status evaluation through **A** epigenomics road-map project, **B** KEGG 2021 Human, **C** proteomic signature through Reactome 2022, **D** CHEA3 gene signature density-based heat map density mapping transcription factor, **E** IPA pathway analysis showing respective interactions. Orange annotation: significant, blue annotation: non-significant

database, showed enrichment of voltage gated ion-channel mediated pathways, particularly, hyper-methylation of potassium (*KCNA3*, and *KCNA6*) and calcium (*CACNB2*) ion channels in PDAC. These genes were further assessed through (i) epigenomics roadmap project, showing most significant correlation with DNA packaging protein, histone 3 (H3K27meH9) (Fig. 1A), (ii) KEGG 2021 Human showing most significant correlation with progesterone mediated oocyte maturation (Fig. 1B), and (iii) Reactome 2022 showing most significant correlation with g2 phase r-hsa-68911 (Fig. 1C) pathway, using Enrichr, online web tool. p -value < 0.05 was considered as a significant enrichment. mRNA expression of these gDMs were analyzed through CHEA3 density based heatmap (Fig. 1D). Ingenuity pathway analysis (IPA) using IPA software (version 42,012,434; Ingenuity Systems; Qiagen China Co., Ltd.), showed global profiles of signaling pathways, functions and interactions associated with these 91 gDMs (Fig. 1E).

3.2 Clinical relevance of significant differentially methylated genes.

Metascape data from our previous study [14] and IPA analysis resulted in identification of 7 'ion transport regulation' associated gDMs: *RASA3*, *CLIC5*, *KCNA3*, *KCNA6*, *KCNJ5*, *CACNB2* and *GABRR2*. Pan cancer profiling of these gDMs were done targeting all cancer subtypes (tumor vs normal) (Supplemental Fig. 1). Expression profile of *KCNJ5*, *KCNA3*, *CLIC5*, *CACNB2*, and *GABRR2* genes, assessed through GTEx (normal database) targeting all 32 tissue types, demonstrated low expression of *KCNJ5*, *CACNB2* and *RASA3*, while the rest, *CLIC5*, *KCNA3*, *KCNA6* and *GABRR2* showed negligible expression in normal pancreas, (Supplemental Fig. 2).

Differential mRNA expression in pancreatic tumor (TCGA dataset) and normal pancreas (GTEx dataset) using Wilcoxon signed rank test showed significant elevated expressions of *KCNJ5* (Fig. 2A) and non-significant high expression of *CACNB2* (Supplemental Fig. 3A) in normal pancreas with respect to PanCa, whereas, *RASA3* (Fig. 2B) and *CLIC5* (Fig. 2C) showed significant over-expression in PanCa in comparison to that of normal pancreas. *KCNA3* was also over-expressed (not significant), in PanCa (Supplemental Fig. 3B). Extent of methylation of both *CACNB2* and *KCNJ5* was significantly higher in PanCa tissue as compared to that of normal pancreas (Fig. 2D, E) in TCGA cohort. Gene expression of *KCNJ5*, *KCNA6* and *GABRR2* showed no significant correlation with methylation in TCGA cohort. *CACNB2*, *CLIC5* and *KCNA3* showed negative correlation between methylation and gene expressions with R -values of -0.43 , -0.16 , and -0.52 respectively. Only *RASA3* expression showed a non-significant positive correlation with methylation (R -value = 0.12) (Supplemental Fig. 4). Stage-wise expression of *CACNB2* and *GABRR2* genes showed significant over-expression with advancement of PanCa stages, I-IV, while, *KCNJ5* showed only marginal upregulation (Supplemental Fig. 5). Assessing *Kcnj5* protein (Kir

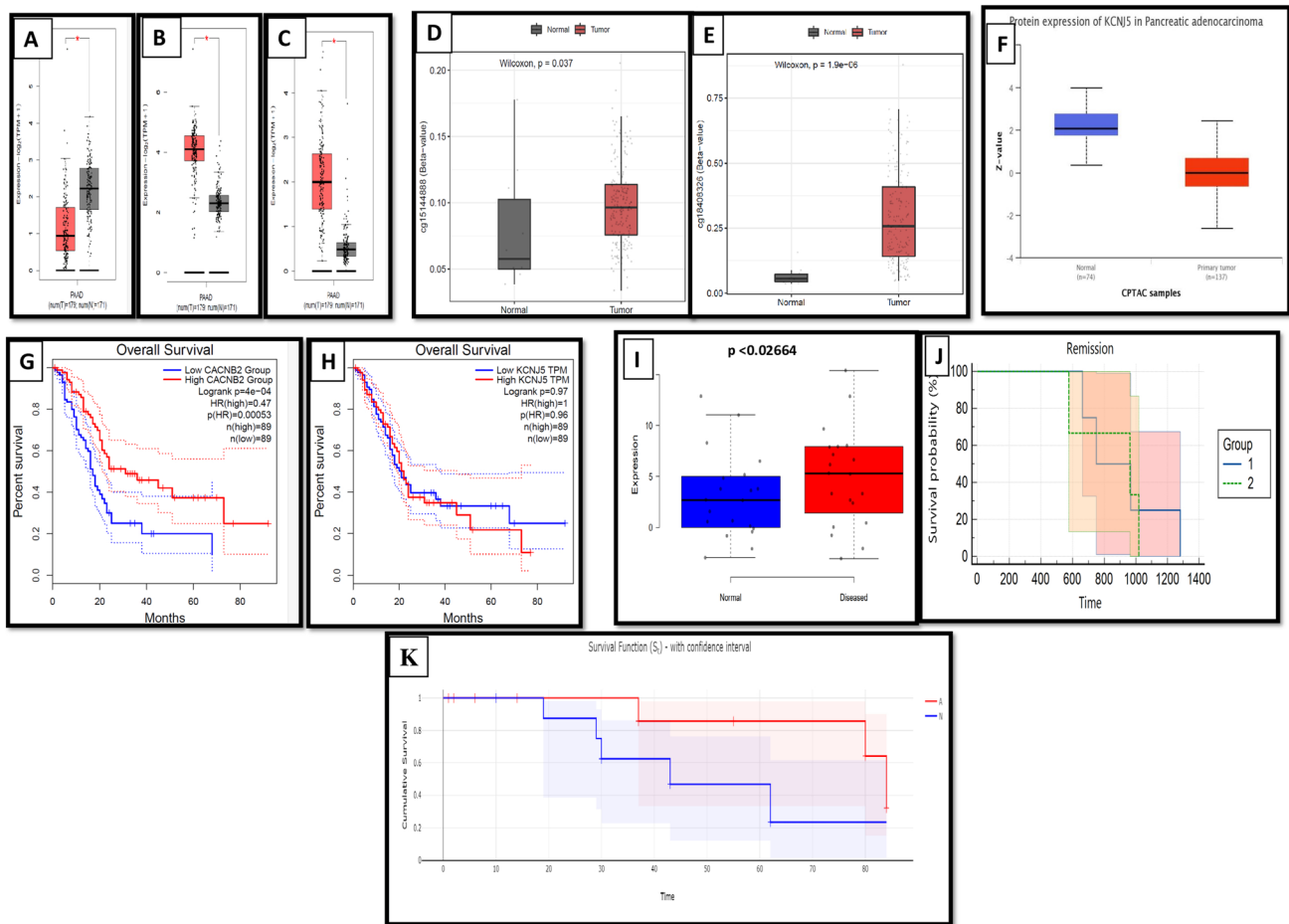


Fig. 2 Clinical relevance of significant differentially methylated genes. Differential expression (TCGA, tumor Vs GTEx, normal) of **A** *KCNJ5* **B** *RASA3* **C** *CLIC5*. Differential methylation pattern of *KCNJ5* (**D**), *CACNB2* (**E**) (TCGA, tumor Vs TCGA, normal) using Wilcoxon Ranksum test; $p=0.037$. **F** *Kcnj5* protein expression was evaluated in CPTAC patient samples (tumor vs normal). Overall survival shown through Kaplan Meyer plot across TCGA patient samples post splitting the samples in low and high risk groups for **G** *CACNB2*, $p=4e-04$, **(H)** *KCNJ5*, $p=0.97$. **I** Differential expression of *KCNJ5* on PDAC paired tumor samples ($n=20$, $p<0.0264$). **J** Overall survival using Kaplan Meier survival analysis of *KCNJ5* using gene expression data done on 20 patient samples in Indian cohort (1 = high *KCNJ5* group, 2 = low *KCNJ5* group). Time is measured in days. **K** KM done between the alcohol and non-alcoholic groups and was found to be border line significant ($p<0.07$)

3.4) expression evaluated through CPTAC in patient samples (tumor vs normal) demonstrated its down-regulation in PDAC in comparison to normal pancreas (Fig. 2F). Mutational status of these 7 genes, assessed through cBioPortal (TCGA, Firehose Legacy) showed missense mutation of all the 7 genes in PDAC. *CACNB2* and *GABBR2* showed deep deletion, while, *KCNA6* demonstrated amplification in PDAC along with missense mutation (Supplemental Figs. 6 and 7). Kaplan–meier survival curves, showed that OS of low *CACNB2* group conferred poor prognosis as compared to high *CACNB2* group (Fig. 2G), while OS of both high and low *KCNJ5* groups were comparable (Fig. 2H).

3.3 *KCNJ5* expression validation using SyBr green method and Kaplan–meier OS analysis

Literature based primers of *KCNJ5* were used to screen 20 PDAC samples. Post normalization, *GAPDH* was used as a housekeeping gene to compare tumor and normal pancreas data. Over-expression of *KCNJ5* was shown in tumor as compared to normal pancreatic tissue in Indian PanCa cohort (Fig. 2I). OS within high and low *KCNJ5* group, in Indian PanCa cohort showed significant difference ($p=0.0019$), with high *KCNJ5* group showing a drop in good prognosis as compared to low *KCNJ5* group around the mid of survival probability mark in the graph (Fig. 2J). Kaplan–meier was done also post comparison between the alcohol and non-alcoholic groups and was found to be border line significant ($p<0.07$) (Fig. 2K). OS of both high and low *CLIC5*, *RASA3* and *KCNA3* group were comparable, while low *GABBR2* group

showed adverse prognosis as compared to high *GABBR2* group (Supplemental Fig. 3C–F). OS was calculated considering a confidence Interval of 95% as standard.

Further validation of *KCNJ5* expression using 3 publicly available GEO datasets, observations showed association of hypermethylation with down-regulation (fold change -1.9) in concordance with findings of TCGA dataset. *KCNJ5* expression status when checked via another dataset namely GSE 16515, we found it to be significantly downregulated which is in concordance with our TCGA and other GEO datasets observations (Supplemental Table 1).

3.4 Correlation of immune cell with differentially methylated genes

Immune profiling using LM22 cell types of *KCNJ5* (Fig. 3A), *CACNB2* (Fig. 3B) revealed a positive correlation between both *KCNJ5* and *CACNB2* with resting mast cells, while showed negative correlation with undifferentiated macrophage (M0) and memory B cells. *KCNJ5* showed a positive correlation with CD8 + T cells, CD4 + memory T cells, pro-inflammatory macrophages (M1), while *CACNB2* was positively correlated with activated NK cells, anti-inflammatory macrophages (M2) and activated mast cells. A negative correlation was observed in case of *KCNJ5* and dendritic and activated mast cells. Also, *CACNB2* showed negative correlation with regulatory T cells. Additionally, a positive correlation is shown between *KCNJ5* and TAMs, which acted as a tumor suppressor, mediated by the release of pro-inflammatory cytokines and tumor necrosis factors (Fig. 3A, 3B). T cells, M1 Macrophages and NK cells are forerunners within the immune system hence their dysregulation acts as crucial regulator for disease progression. These positive correlations are potential identifiers

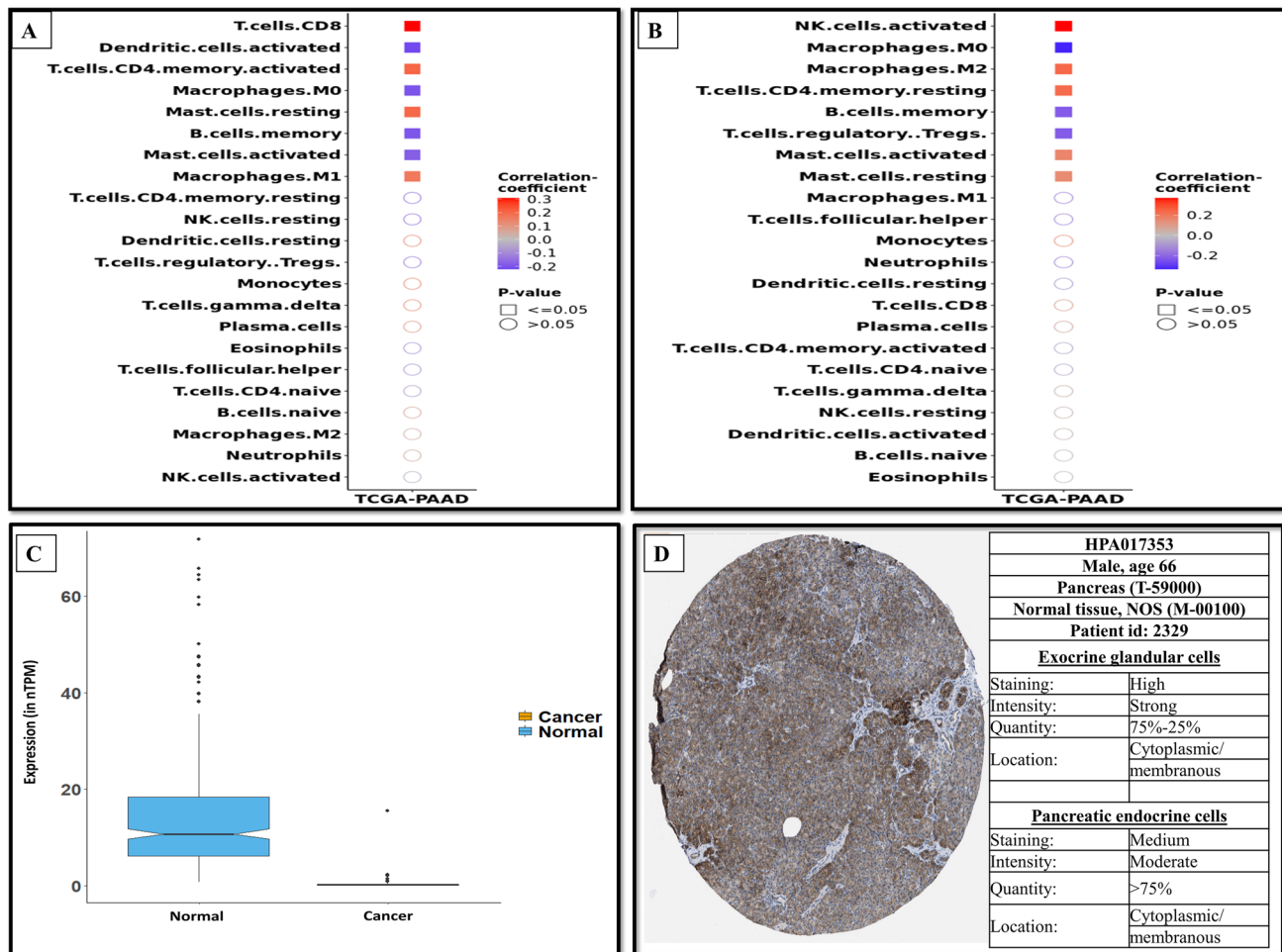


Fig. 3 Deconvolution immune profiling using LM22 for **A** *KCNJ5*, **B** *CACNB2* expression correlation in different immune cells. Correlation coefficient is denoted by blue to red. Blue denoting negative correlation, red denoting positive correlation. Expression of *KCNJ5* in Human Protein Atlas **C**. Whisker plot comparing the RNA expression (in nTPM) of *KCNJ5* in 328 GTEx normal pancreatic tissue samples and 46 pancreatic cancer cell lines **D**. Immunohistochemistry of *KCNJ5* in normal pancreatic tissue

of disease associated immune cells upregulation and hence are suitable immune therapy targets for controlling disease associated immune microenvironment dysfunction along with disease manifestations.

3.5 Cross-validation of *KCNJ5* expression in HPA database

On comparing the gene expression of *KCNJ5* in normal and PanCa cell lines, it was found that the mean nTPM value is 14.5 and 0.6 for normal pancreatic tissue and PanCa respectively (Fig. 3C). Immunohistochemistry results showed that *KCNJ5* is highly and moderately expressed at protein level in normal exocrine and endocrine cells of pancreas respectively (Fig. 3D). Hence, *KCNJ5* showed low expression in PanCa compared to normal pancreatic tissue.

3.6 Functional network analysis of *KCNJ5*

Using an interaction score threshold of 0.7 (high confidence), the STRING PPI analysis (Fig. 4A–C) resulted a highly clustered network, indicating significantly more interaction than expected for a random set of similar size drawn from the genome (enrichment p-value < 0.001). Enrichment analysis of *KCNJ5* based on PPI using GO, showed significant involvement of inwardly rectifying potassium channel subfamily J: *KCNJ3*, *KCNJ5*, *KCNJ6*, *KCNJ9* and *KCNJ15*, G protein subunit γ and γ aminobutyric acid type B receptor subunit 2 components in GO biological pathways (Fig. 4A), molecular functions (Fig. 4B) and cellular components (Fig. 4C) terms in the network. Similar enrichment analysis of *KCNJ5* in our Indian cohort [14] using GO, depicted concordant observations in GO biological pathways (Fig. 4D).

3.7 Functional enrichment of *KCNJ5* and associated co-expressed genes

Linked-Omic, based functional and pathways enrichment analysis of *KCNJ5* and its associated genes in a cohort of 178 patients, having total 19,774 genes were enriched in this study, of them, 11,057 genes showed negative correlations, while the remaining 8717 genes showed significant positive correlation with *KCNJ5* (Fig. 5A). The most positive and negative correlated genes associated with *KCNJ5* are represented in the heatmap (Fig. 5B and C). For functional enrichment of the correlated genes with *KCNJ5*, enrichment studies were executed using Gene Set Enrichment Analysis (GSEA)

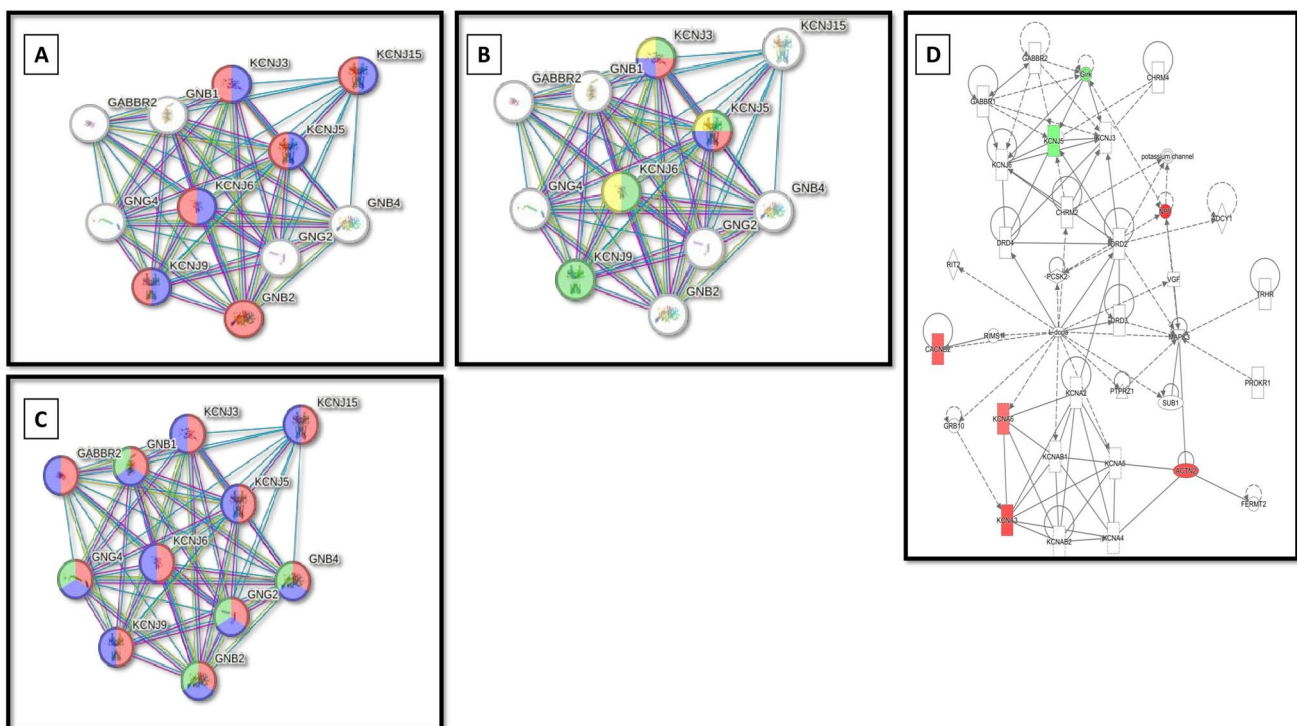


Fig. 4 Functional validation of *KCNJ5* gene. Gene Ontology based on **A** biological processes using STRING **B** molecular functions **C** cellular components. **(D)** Interaction between all ion channel genes, including *KCNJ5*, *CACNB2*, *KCNA3*, *KCNA6*, *GABBR2*

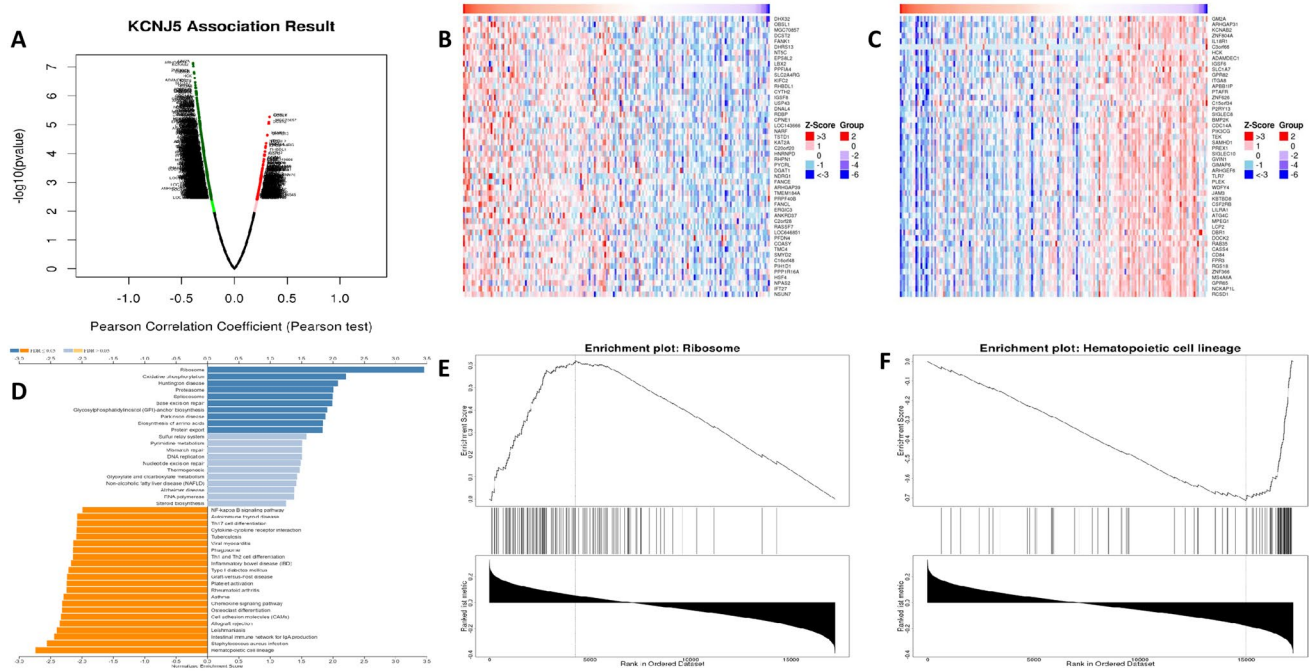


Fig. 5 Functional enrichment of *KCNJ5*: **A** Volcanic graph of *KCNJ5* representing positive (red) and negative (green) correlated genes. **B** Heatmap of *KCNJ5* associated positive correlated genes. **C** Heatmap of *KCNJ5* associated negative correlated genes. **D** Functional and pathways enrichment analysis of *KCNJ5* associated positive (blue) and negative (yellow) correlated genes. **E** Enrichment plot for ribosome associated pathways. **F** Enrichment plot for hematopoietic cell lineage pathways

method and KEGG pathways category in the Link-Interpreter submodule of Linked-Omics. As exhibited in Fig. 5D, the *KCNJ5* correlated genes show a positive association with oxidative phosphorylation, DNA repair, proteasome, spliceosome related pathways, etc. with ribosome linked pathways, being the most prominent. While, IgA production Th 1,2,17 differentiations, chemokine signaling etc. showed negative association of *KCNJ5*, with hematopoietic cell lineage pathways showing most negative association. The enrichment plot of ribosome-associated (Fig. 5E) and hematopoietic cell lineage (Fig. 5F) pathways were demonstrated.

3.8 Identification of differentially expressed ion channel genes (DEICG) for PDAC and protein–protein interaction enrichment analysis

A list of 8208 DEGs obtained by combining the results from GSE211398 and GSE93326 and TCGA, was further analyzed to acquire 129 DEICGs. The expression (\log_2FC) of 41 up-regulated and 88 down-regulated DEICGs are shown in Fig. 6A. Next, we generated a protein–protein interaction network (PPIN) of DEICGs in Metascape. Subsequently, the functional enrichment and MCODE cluster analysis of this PPIN (Fig. 6B–D) in Metascape showed that GO:0098660 (inorganic ion transmembrane transport) is the most enriched GO Biological Process and there are 8 significant clusters in this PPIN (Fig. 6D).

3.9 Revalidation of methylation status in 450 K dataset from Indian cohort

To further validate our observations concerning methylation status of seven genes, we utilized our own dataset GSE181740 with PanCa patient population of Indian origin. *KCNJ5*, *CLIC5*, *GABBR2*, and *RASA3* were found to be hypomethylated and *CACNB2*, *KCNA3*, while *KCNA6* were hypermethylated based on the delta beta value, obtained post normalization using 450 K methylome array (Supplementary Fig. 8). However, all together in Indian cohort of PanCa, *CANNB2*, *KCNA3* and *KCNA6* were hyper-methylated, while *KCNJ5*, *CLIC5*, *GABRR2* and *RASA3* were hypo-methylated (Supplemental Fig. 8).

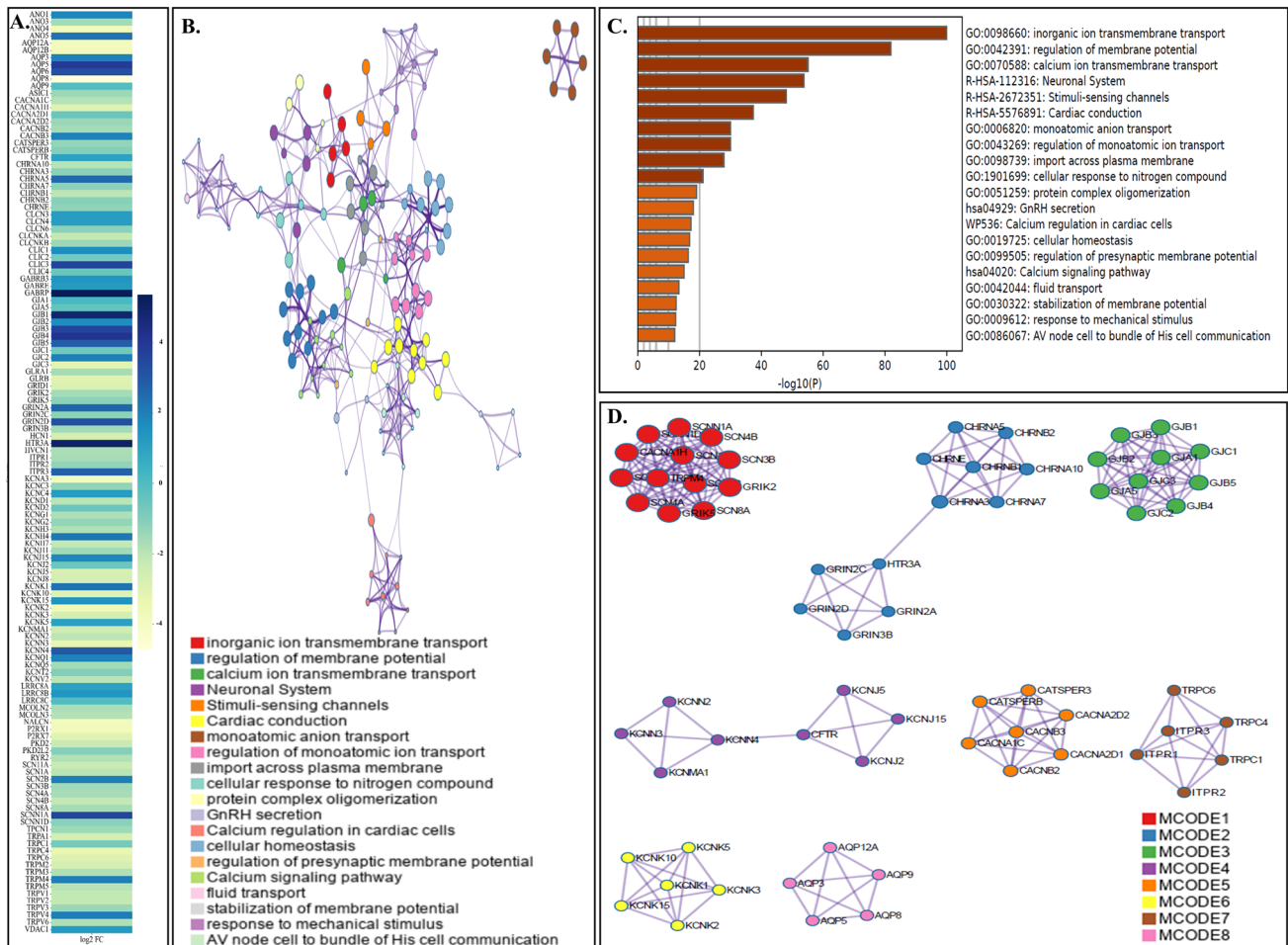


Fig. 6 Identification, functional enrichment and cluster analysis of protein–protein interaction network of DEICGs in PDAC. **A** Heat map depicting the average gene expression (log₂FC) of 129 DEICGs in three datasets –GSE211398, GSE93326 and TCGA. **B** Functional enrichment network of DEICGs that is cluster ID-colored, with nodes with the same cluster ID being closer to one another. **C**. Bar plot of Top 20 significant GO Biological Processes and KEGG pathways of DEICGs. **D**. MCODE clusters identified in the network of protein–protein interactions of DEICGs.

3.10 Transcription factors regulate the expression of *KCNJ5*

By combining the TF-binding data of ChEA and RegNetwork, we identified two transcription factors, *POU2F1* and *POU3F1*, both of which might regulate the overexpression of *KCNJ5* in PanCa.

3.11 ScRNA seq based validation of *KCNJ5* cell type specific expression.

ScRNA-seq studies, based on TCGA database, showed elevated expression of *KCNJ5* in macrophage (~ threefold) and naïve B cells (~ twofold), in comparison with malignant cells in PanCa (Supplemental Fig. 9).

3.12 *KCNJ5* expression in various pancreatic cancer cell lines

The CCL DepMap portal showed that median expression of *KCNJ5* is low across 50 PanCa cell lines (Supplementary Fig. 10A). But, on examining its expression in individual PanCa cell line in CCL DepMap portal it was found that, *KCNJ5* is significantly over-expressed in SU86.86, YAPC and HUPT4 PanCa cell line (Supplemental Fig. 10B.), while

no cell line documented its protein level expression so far. Similarly, Human Protein Atlas also showed that *KCNJ5* is overexpressed in SU86.86, YAPC and HUPT4 (Supplemental Fig. 10C). It is of interest to note that the origin of SU86.86 is from Caucasian population while that of YAPC and HUPT4 are from Asian population.

3.13 Identification of small molecule/ drugs targeting Kcnj5

Several small molecule/ drugs targeting Kcnj5 identified through CMap database based on their high enrichment score are Amiloride (enrichment score 1.31) and Vernakalant hydrochloride (enrichment score 1.97) (Supplemental Table 2). FDA approved, Amiloride is a sodium ion channel blocker, while, sodium and potassium ion channel blocker, Vernakalant hydrochloride, is not approved by FDA. However, Vernakalant hydrochloride (enrichment score 1.97) is approved by European Medicines Agency and in regular clinical practice in European Union and the United Kingdom since 2010. Few other small molecules/ drugs targeting Kcnj5, identified through depmap portal are [Dalfampridine](#), [Glyburide](#) and [Levcromakalim](#). Potassium channel blocker, [Dalfampridine](#), and second generation sulfonylurea and ATP channel blocker, [Glyburide](#) are approved by FDA. However, potassium channel activator, Levcromakalim is under clinical assessment through trial studies.

3.14 Virtual screening of potential ligands for Kcnj5 protein

Among the evaluated ligands, protodioscin, a steroidal saponin, exhibited the most favorable Glide score (-9.147 kcal/mol), indicating the strongest binding affinity for Kcnj5 (refer to Supplemental Table 3). Detailed molecular docking analysis unveiled specific interactions and a complex interplay of various chemical forces between protodioscin and the amino acid residues within the Kcnj5 binding site (Fig. 7A, B). The central steroidal backbone of protodioscin, flanked by multiple rings, engaged in π -alkyl interactions predominantly with His A:64 and Ala A:197. Additionally, conventional hydrogen bonds formed between critical hydroxyl groups and residues such as Asp A:83, Gln A:192, Arg A:319, and Glu A:55 further stabilized the ligand–protein complex. Van der Waals interactions with Ala A:318 and Val A:175 also contributed to the enhanced binding affinity.

The hydrogen bond donor–acceptor map (Fig. 7C) highlighted the crucial roles of Glu A:55 and Thr A:80 in establishing hydrogen bonds. Hydrophobicity analysis (Fig. 7D) underscored the hydrophobic nature of the binding pocket, with significant interaction regions aligning with hydrophobic residues like Leu A:84 and Pro A:193. Moreover, the ionizability landscape (Fig. 7E) revealed a predominance of acidic environments, evidenced by residues such as Glu A:55 and Asp A:83.

A 100-ns molecular dynamics (MD) simulation of the protodioscin-Kcnj5 protein complex provided comprehensive insights into its stability and structural dynamics (Supplemental Fig. 11). Initial conformational adjustments were observed, with root mean square deviation (RMSD) values stabilizing around 20 ns, averaging 7.67 ± 1.12 Å, which indicated a stable binding interaction. The root mean square fluctuation (RMSF) plot showed that residues at the binding site, which interact with protodioscin, exhibited lower fluctuations, signifying stabilized regions due to ligand binding. Collectively, these results confirm the dynamic stability and structural integrity of the protodioscin-Kcnj5 protein complex, underscoring the potential of protodioscin as a promising therapeutic candidate for targeting Kcnj5 in PanCa.

4 Discussion

Based on 450 K methylome data, a previous study from our group showed that epigenetic and genetic signatures of Indian cohort of PDAC patients diverge partially based on expression frequency and alternated driver behaviors, across the globe. This wide variation in methylation landscape between TCGA, and our cohort, included 156 differentially methylated positions annotated to 91 genes having differential methylation (gDMs). Similarly, our previous data also showed variance in various parameters like, *KRAS* mutation frequency, *NPY* and *FAIM2* differential methylation pattern in Indian PDAC samples and Indian data were different with respect to western patient cohort [26]. The possible reason of this variability were ethnicity, environment, lifestyle and occupational hazards. Enrichment analysis using GO/KEGG terms, canonical pathways and hall mark gene sets and network analysis of these 91 gDMs, pointed “regulation of ion transport”, as the most statistically significant enriched term [17]. Metascape data from our previous study and IPA data from this study resulted in the identification of 7 ‘ion transport regulation’ associated gDMs: *RASA3*, *CLIC5*, *KCNA3*, *KCNA6*, *KCNJ5*, *CACNB2* and *GABRR2*. Significant differential expression in normal tissue samples in GTEx cohort versus cancer samples in the TCGA cohort was shown in case of *RASA3*, *KCNJ5* and *CLIC5*, while that of *CACNB2* was not significant.

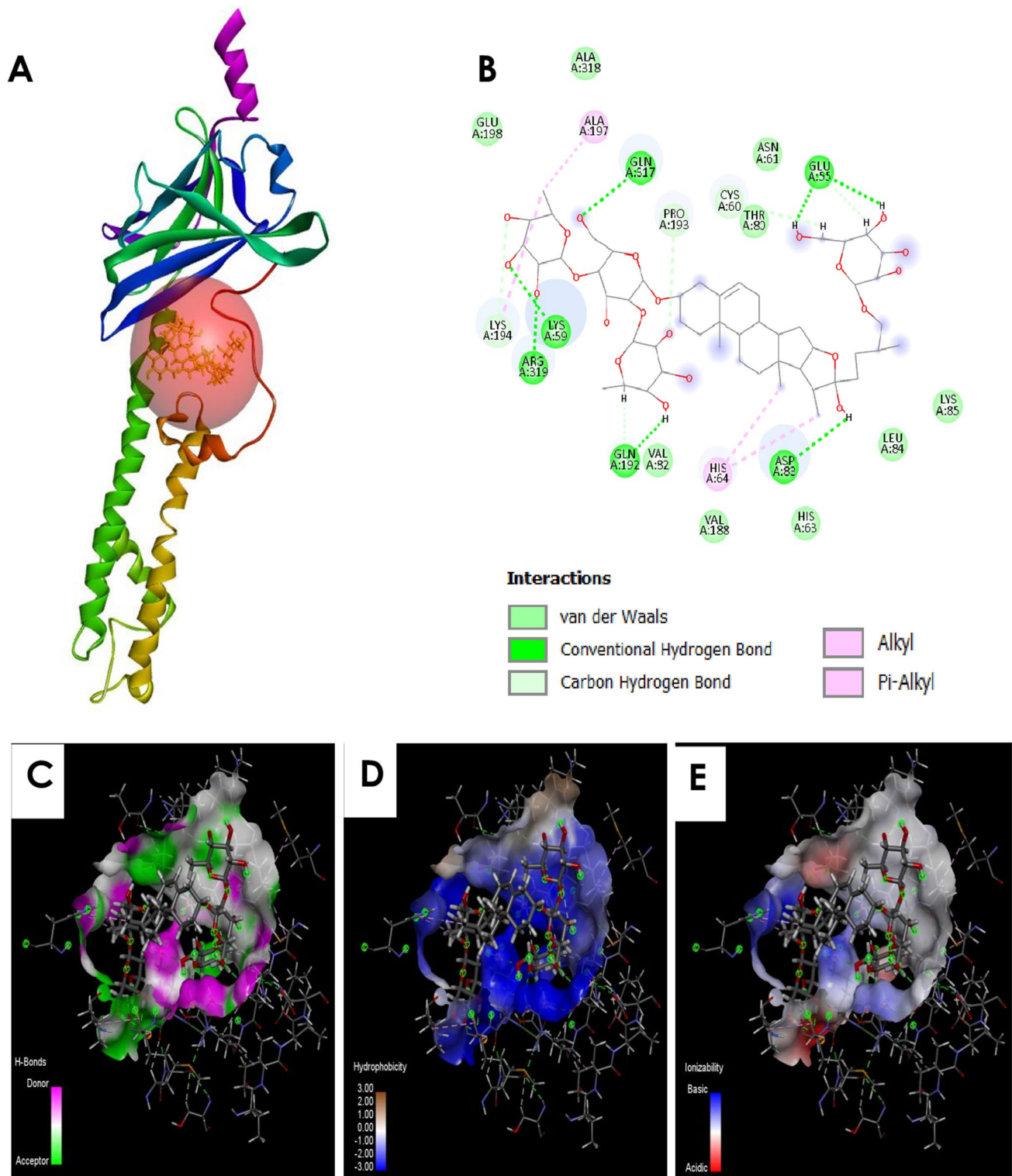


Fig. 7 Molecular docking study of protodioscin to the modelled Kcnj5 protein. **A** 3D diagram of the complex. **B** 2D diagram of interactions of the ligand with the amino acid residues at the binding site. **C–E** Mapping of binding site cavity according to the presence of H-bond donor–acceptor residue, hydrophobicity, and ionizability, respectively

KCNJ5, was hypomethylated and overexpressed in our Indian cohort [17] while hypermethylated and underexpressed in the TCGA cohort. Kaplan–Meier survival data of Indian cohort also showed significant poor survival in high *KCNJ5* group as compared to low *KCNJ5* group. This finding is further strengthened by its over-expression significantly in PanCa cell

lines, SU86.86, YAPC and HuP T4, while its protein, Kir3.4 expressions is not demonstrated in any cell lines so far (Supplemental Fig. 9), showing concordance with TCGA based *KCNJ5* expression patterns.

KCNJ5, coding for inward rectifying potassium channel protein, Kir3.4 is regulated by G proteins, usually detected at low levels in normal pancreas. Kir channels are associated with heart rate, hormone secretion, renal functions, atrial fibrillation, hypertension, and type II diabetes [27]. Similarly, Ca²⁺ Voltage-Gated Channel Auxiliary Subunit Beta 2 (*CACNB2*) is mutated in lung cancer [28] and Hodgkin lymphoma [29] and showed chemoresistance in esophageal squamous cell carcinoma, while suppressed head and neck squamous cell carcinoma [30, 31].

Various kinds of Kir channels are associated with all the hallmarks of cancer in vast array of malignancies. A group-member, Kir3.4 (*KCNJ5*) promoted cell proliferation in aldosterone-producing adenoma. It showed association with restructuring of immune microenvironment in colon cancer, facilitating G-protein/ phospholipase C/ DAG mediated M2 macrophage infiltration and recruitment both in vitro and in vivo (xenograft animal models) [32]. However, our LM22 based immune profiling data (Fig. 3) demonstrated a positive correlation with M1 TAMs, acting as a tumor suppressor, mediated by the release of pro-inflammatory cytokines and tumor necrosis factors. *KCNJ5* boosted the aggressiveness of triple-negative breast cancer and was elevated in MGC-803, gastric cancer cells [33, 34]. Similarly, we documented the upregulation of *KCNJ5* in our Indian PanCa cohort, showing its credibility as a drug target in these devastating diseases.

Findings of both the TCGA based studies; (i) ScRNA-seq study, showing elevated expression of *KCNJ5* in macrophage and naïve B cells, while diminished levels in pancreatic malignant cells (Supplement Fig. 9) and (ii) low bulk tissue expression of *KCNJ5* in PanCa tissue (Fig. 2) are in concordance.

Two TFs of *KCNJ5* that were identified in our study are *POU2F1* and *POU3F1*. It was found that there is a connection between developmental homeodomain/POU domain transcription factors and cancer cell metabolism. Literary evidences deciphered that *POU2F1* is significantly over-expressed in gastric cancer, colon cancer. Whereas, this TF was found to be therapeutic against lung cancer. The TF *POU3F1* on the other hand was reported to reduce ROS (Reactive Oxygen Species), DNA damage response (DDR), and senescence in H460 non-small-cell lung carcinoma cells. Thus, the regulation of *KCNJ5* through modification of *POU2F1* and *POU3F1*, could help in devising advanced therapeutic strategies against the disease.

Our study predicted that onco-channel *KCNJ5* can be targeted by several other ion channel blockers, Amiloride, Vernakalant hydrochloride, Dalfampridine, Glyburide and Levcromakalim. Among these, antikaliuretic-diuretic, Amiloride, synergized the chemosensitivity of (i) Erlotinib in Bxpc-3 and PANC-1 PanCa cells and (ii) Sunitinib in renal cancer Caki-1 cells [35, 36]. It also suppressed growth and proliferation of H6 hepatoma cells, and induced apoptosis in cell line and animal models of multiple myeloma [37, 38]. Anti-diabetic drug, Glibenclimide also showed anti-neoplastic effects. Thus, these predicted synthetic anti-Kcnj5 compounds demand further assessment for their therapeutic potential in Indian patients' suffering from PanCa [39]. Naturally derived, steroidal saponin, protodioscin and its derivatives suppressed prostate cancer, bladder cancer and oral cancer [40–42]. The virtual screening identified protodioscin as a potent ligand for Kcnj5, the upregulated oncochannel in Indian PanCa (Fig. 6). The favorable binding interactions and dynamic stability of the protodioscin-Kcnj5 complex provide a strong rationale for further evaluation of protodioscin as a novel therapeutic targeting this crucial ion channel [43].

PanCa, a highly aggressive disease, progresses rapidly and resist available treatments, leading to devastating outcome. Though numerous studies are highlighting the intricate mechanisms of disease progression, translation of this knowledge into PanCa therapy is lacking. Thus, novel concepts in this field are the only way out. Embedded on cell membrane, ion-channels are able to alter tumor and its microenvironment through manipulating various signaling cascades. Externally located ion channels make them an attractive and ideal drug target. Thus, our data demonstrating over-expression of Kcnj5 can be probably targeted in disease management of Indian PanCa patients. The small sample size (n = 20) of our Indian cohort, indicating the association of enhanced *KCNJ5* with PanCa, however needs to be confirmed in a larger cohort couple with immunohistochemistry and further functional studies in PanCa cell lines.

5 Conclusion

Owing to the critical and complex role of potassium ion channels in cancer signaling pathways, *KCNJ5*, identified as a novel oncochannel overexpressed and associated with relative poor patient survival in Indian cohort of PanCa, shows that it might have some play in disease physiology subjective to further validation. Probably several lines of therapeutic strategies specific for Indian patient population that can be developed based on our findings are (i) targeting two TFs *POU2F1* and *POU3F1* controlling the expression of *KCNJ5*, (ii) prediction of Amiloride, Vernakalant hydrochloride, Dalfampridine, Glyburide and Levcromakalim as small molecules acting as anti-Kcnj5 and (iii) targeting Kcnj5 with natural

product protodioscin. The role of *KCNJ5* is also demographic/ethnicity specific which is validated across several observations and this uplifts the role of biomarker development specific to our population. The data would help to develop remedial measures in facilitating PanCa management in Indian patients.

Acknowledgements The authors deeply acknowledge all the database-generating labs and associated teams for maintaining a structured database. Authors appreciate Dr. Gourab Saha, ThermoFisher Scientific lab, and Dr. Ankita Chatterjee, National Institute of BioMedical Genomics, for their moral input. The authors also expressed their gratitude to Dr. Paromita Roy, Tata Medical Centre and Dr. Sankhyadeep Dutta, CNCI, Kolkata for being the backbone of the study. The authors thank Dr. Meenakshi Munshi, Department of Biotechnology, GOI, for supporting and processing the fund. N.S. also thanks to Master. Saraswan Sikdar.

Author contributions A.B curated the raw datasets for downstream analysis followed by collection of clinical data and specimens from respective hospitals, and wet lab data generation. A.M and D.D analyzed the data, wrote and arranged figures and tables for the original manuscript. D.G.D and G.G did the in silico virtual screening and manuscript writing. S.M did scRNA validation along with proofread and edited the entire manuscript along with data result validation. Shi.G., B.K. C,S.B., and Sup.G. gave the clinical data and pancreatic tumor tissue samples from respective hospitals. N.S. designed, conceptualized, validated, edited, revised, and correspond the manuscript.

Funding The study was supported by the Department of Biotechnology (DBT), Government of India (GOI) Grant Sanction Number: Ramalingaswami Re-entry fellowship (RLS/BT/Re-entry/05/2012).

Data availability Data available on reasonable request.

Declarations

Ethics approval and consent to participate The authors sincerely thank the participants for their help and willingness to take part in this study. Patient samples were collected from two State Government Hospitals (Medical College & Hospital, Kolkata, SSKM & I.P.G.M.E.&R Hospital, Kolkata), Government of West Bengal, and three private hospitals, Calcutta Medical Research Institute (CMRI), C. K. Birla Hospital and Tata Medical Center (TMC), Rajarhat, Kolkata. The study was approved by the Institutional Review Board (IRB) of Indian Statistical Institute, Kolkata and also from all the above-mentioned Hospitals. The consents were taken from each patient and their families for this study.

Consent for publication No individual person's data were used in this study.

Competing interests The authors declare no competing interests.

Open Access This article is licensed under a Creative Commons Attribution-NonCommercial-NoDerivatives 4.0 International License, which permits any non-commercial use, sharing, distribution and reproduction in any medium or format, as long as you give appropriate credit to the original author(s) and the source, provide a link to the Creative Commons licence, and indicate if you modified the licensed material. You do not have permission under this licence to share adapted material derived from this article or parts of it. The images or other third party material in this article are included in the article's Creative Commons licence, unless indicated otherwise in a credit line to the material. If material is not included in the article's Creative Commons licence and your intended use is not permitted by statutory regulation or exceeds the permitted use, you will need to obtain permission directly from the copyright holder. To view a copy of this licence, visit <http://creativecommons.org/licenses/by-nc-nd/4.0/>.

References

1. Bararia A, Das A, Mitra S, Banerjee S, Chatterjee A, Sikdar N. Deoxyribonucleic acid methylation driven aberrations in pancreatic cancer-related pathways. *World J Gastrointest Oncol.* 2023;15:1505–19.
2. Sikdar N, Saha G, Dutta A, Ghosh S, Shrikhande SV, Banerjee S. Genetic alterations of periampullary and pancreatic ductal adenocarcinoma: an overview. *Curr Genomics.* 2018;19:444–63.
3. Bararia A, Dey S, Gulati S, Ghatak S, Ghosh S, Banerjee S, et al. Differential methylation landscape of pancreatic ductal adenocarcinoma and its precancerous lesions. *Hepatobiliary Pancreat Dis Int.* 2020;19:205–17.
4. Bararia A, Chakraborty P, Roy P, Chattopadhyay BK, Das A, Chatterjee A, et al. Emerging role of non-invasive and liquid biopsy biomarkers in pancreatic cancer. *World J Gastroenterol.* 2023;29:2241–60.
5. Prevarskaya N, Skryma R, Shuba Y. Ion channels in cancer: are cancer hallmarks oncochannelopathies? *Physiol Rev.* 2018;98:559–621.
6. Jiang L-H, Adinolfi E, Roger S. Editorial: ion channel signalling in cancer: from molecular mechanisms to therapeutics. *Front Pharmacol.* 2021;12: 711593.
7. Altamura C, Gavazzo P, Pusch M, Desaphy J-F. Ion channel involvement in tumor drug resistance. *J Pers Med.* 2022;12:210.
8. Hofschroer V, Najder K, Rugi M, Bouazzi R, Cozzolino M, Arcangeli A, et al. Ion channels orchestrate pancreatic ductal adenocarcinoma progression and therapy. *Front Pharmacol.* 2020;11: 586599.
9. Zúñiga L, Cayo A, González W, Vilos C, Zúñiga R. Potassium channels as a target for cancer therapy: current perspectives. *Onco Targets Ther.* 2022;15:783–97.
10. Patel SH, Edwards MJ, Ahmad SA. Intracellular ion channels in pancreas cancer. *Cell Physiol Biochem.* 2019;53:44–51.
11. Schnipper J, Dhennin-Duthille I, Ahidouch A, Ouadid-Ahidouch H. Ion channel signature in healthy pancreas and pancreatic ductal adenocarcinoma. *Front Pharmacol.* 2020;11: 568993.

12. Huang X, Jan LY. Targeting potassium channels in cancer. *J Cell Biol.* 2014;206:151–62.
13. Becchetti A, Petroni G, Arcangeli A. Ion channel conformations regulate integrin-dependent signaling. *Trends Cell Biol.* 2019;29:298–307.
14. Hu D, Ansari D, Bauden M, Zhou Q, Andersson R. The emerging role of calcium-activated chloride channel regulator 1 in cancer. *Anticancer Res.* 2019;39:1661–6.
15. Bettaieb L, Brulé M, Chomy A, Diedro M, Fruit M, Happerneegg E, et al. Ca²⁺ signaling and its potential targeting in pancreatic ductal carcinoma. *Cancers.* 2021;13:3085.
16. Yee NS. TRPM8 ion channels as potential cancer biomarker and target in pancreatic cancer. *Adv Protein Chem Struct Biol.* 2016;104:127–55.
17. Chatterjee A, Bararia A, Ganguly D, Mondal PK, Roy P, Banerjee S, et al. DNA methylome in pancreatic cancer identified novel promoter hyper-methylation in NPY and FAIM2 genes associated with poor prognosis in Indian patient cohort. *Cancer Cell Int.* 2022;22:334.
18. Chandrashekar DS, Basha B, Balasubramanya SAH, Creighton CJ, Ponce-Rodriguez I, Chakravarthi BVSK, et al. UALCAN: a portal for facilitating tumor subgroup gene expression and survival analyses. *Neoplasia.* 2017;19:649–58.
19. Barretina J, Caponigro G, Stransky N, Venkatesan K, Margolin AA, Kim S, et al. The cancer cell line encyclopedia enables predictive modeling of anticancer drug sensitivity. *Nature.* 2012;483:603–7.
20. Li Y, Ge D, Lu C. The SMART App: an interactive web application for comprehensive DNA methylation analysis and visualization. *Epigenetics Chromatin.* 2019;12:71.
21. Liu Z-P, Wu C, Miao H, Wu H. RegNetwork: an integrated database of transcriptional and post-transcriptional regulatory networks in human and mouse. *Database.* 2015; 2015.
22. Peng J, Sun B-F, Chen C-Y, Zhou J-Y, Chen Y-S, Chen H, et al. Single-cell RNA-seq highlights intra-tumoral heterogeneity and malignant progression in pancreatic ductal adenocarcinoma. *Cell Res.* 2019;29:725–38.
23. Mao J, Tian Y, Luo N. An ion channel-based prognostic model identified TRPV2 and GJB3 as immunotherapy determinants in pancreatic cancer. *Heliyon.* 2024;10: e27301.
24. Ghosh D, Ghosh Dastidar D, Roy K, Ghosh A, Mukhopadhyay D, Sikdar N, et al. Computational prediction of the molecular mechanism of statin group of drugs against SARS-CoV-2 pathogenesis. *Sci Rep.* 2022;12:6241.
25. Das S, Paul P, Dastidar DG, Chakraborty P, Chatterjee S, Sarkar S, et al. Piperine exhibits potential antibiofilm activity against *Pseudomonas aeruginosa* by accumulating reactive oxygen species, affecting cell surface hydrophobicity and quorum sensing. *Appl Biochem Biotechnol.* 2023;195:3229–56.
26. Saha G, Singh R, Mandal A, Das S, Chattopadhyay E, Panja P, et al. A novel hotspot and rare somatic mutation p.A138V, at TP53 is associated with poor survival of pancreatic ductal and periampullary adenocarcinoma patients. *Mol Med.* 2020;26:59.
27. Hibino H, Inanobe A, Furutani K, Murakami S, Findlay I, Kurachi Y. Inwardly rectifying potassium channels: their structure, function, and physiological roles. *Physiol Rev.* 2010;90:291–366.
28. Tomoshige K, Matsumoto K, Tsuchiya T, Oikawa M, Miyazaki T, Yamasaki N, et al. Germline mutations causing familial lung cancer. *J Hum Genet.* 2015;60:597–603.
29. Liang K, Wang J, Wang Y, Zhou Z, Ge S, Mei S, et al. The histologic, immunohistochemical, and genetic features of classical Hodgkin lymphoma and anaplastic large cell lymphoma with aberrant T-cell/B-cell antigen expression. *Hum Pathol.* 2019;84:309–20.
30. Xie F, Zhang D, Qian X, Wei H, Zhou L, Ding C, et al. Analysis of cancer-promoting genes related to chemotherapy resistance in esophageal squamous cell carcinoma. *Ann Transl Med.* 2022;10:92.
31. Oshima S, Asai S, Seki N, Minemura C, Kinoshita T, Goto Y, et al. Identification of tumor suppressive genes regulated by miR-31–5p and miR-31–3p in head and neck squamous cell carcinoma. *Int J Mol Sci.* 2021;22:6199.
32. Wang Y, Wang Y, Xu C, Liu Y, Huang Z. Identification of novel tumor-microenvironment-regulating factor that facilitates tumor immune infiltration in colon cancer. *Mol Ther Nucleic Acids.* 2020;22:236–50.
33. Li X, Wang B, Tang L, Zhang Y, Chen L, Gu L, et al. GSTA1 expression is correlated with aldosterone level in KCNJ5-mutated adrenal aldosterone-producing adenoma. *J Clin Endocrinol Metab.* 2018;103:813–23.
34. Wang Y, Jiang X-Y, Yu X-Y. BRD9 controls the oxytocin signaling pathway in gastric cancer via CANA2D4, CALML6, GNAO1, and KCNJ5. *Transl Cancer Res.* 2020;9:3354–66.
35. Zheng Y, Yang H, Li T, Zhao B, Shao T, Xiang X, et al. Amiloride sensitizes human pancreatic cancer cells to erlotinib in vitro through inhibition of the PI3K/AKT signaling pathway. *Acta Pharmacol Sin.* 2015;36:614–26.
36. Bai Y, You Y, Chen D, Chen Y, Yin Z, Liao S, et al. Amiloride reduces fructosamine-3-kinase expression to restore sunitinib sensitivity in renal cell carcinoma. *iScience.* 2024;27:109997.
37. Rojas EA, Corchete LA, San-Segundo L, Martínez-Blanch JF, Codoñer FM, Paíno T, et al. Amiloride, an old diuretic drug, is a potential therapeutic agent for multiple myeloma. *Clin Cancer Res.* 2017;23:6602–15.
38. Sparks RL, Pool TB, Smith NK, Cameron IL. Effects of amiloride on tumor growth and intracellular element content of tumor cells in vivo. *Cancer Res.* 1983;43:73–7.
39. Gao R, Yang T, Xu W. Enemies or weapons in hands: investigational anti-diabetic drug glibenclamide and cancer risk. *Expert Opin Investig Drugs.* 2017;26:853–64.
40. Chen Y-R, Wang S-C, Huang S-P, Su C-C, Liu P-L, Cheng W-C, et al. Protodioscin inhibits bladder cancer cell migration and growth, and promotes apoptosis through activating JNK and p38 signaling pathways. *Biomed Pharmacother.* 2022;156: 113929.
41. Hsieh M-J, Lin C-W, Chen M-K, Chien S-Y, Lo Y-S, Chuang Y-C, et al. Inhibition of cathepsin S confers sensitivity to methyl protodioscin in oral cancer cells via activation of p38 MAPK/JNK signaling pathways. *Sci Rep.* 2017;7:45039.
42. Chen J, Qin P, Tao Z, Ding W, Yao Y, Xu W, et al. Anticancer activity of methyl protodioscin against prostate cancer by modulation of cholesterol-associated MAPK signaling pathway via FOXO1 induction. *Biol Pharm Bull.* 2023;46:574–85.
43. Al-Karaghali MA-M, Ghanizada H, Hansen JM, Skovgaard LT, Olesen J, Larsson HBW, et al. Levromakalim, an adenosine triphosphate-sensitive potassium channel opener, dilates extracerebral but not cerebral arteries. *Headache.* 2019;59:1468–80.